American Journal of Nanosciences
2021; 7(1): 28-34
http://www.sciencepublishinggroup.com/j/ajn
doi: 10.11648/j.ajn.20210701.15
ISSN: 2575-484X (Print); ISSN: 2575-4858 (Online)

Optical Band Energy, Urbach Energy and Associated Band Tails of Nano Crystalline TiO_2 Films at Different Annealing Rates

Geoffrey Gitonga Riungu*, Simon Waweru Mugo, James Mbiyu Ngaruiya, Gitonga Mbae John, Nelson Mugambi

College of Pure and Applied Sciences, Department of Physics, Jomo Kenyatta University of Agriculture and Technology, Nairobi, Kenya

Email address:
geoffreyriungu@gmail.com (G. G. Riungu), wawerumugo@jkuat.ac.ke (S. W. Mugo), ngaruyiajm@fsc.jkuat.ac.ke (J. M. Ngaruiya), mbaejoni@gmail.com (G. M. John), nelmug2013@gmail.com (N. Mugambi)

*Corresponding author

To cite this article:
Geoffrey Gitonga Riungu, Simon Waweru Mugo, James Mbiyu Ngaruiya, Gitonga Mbae John, Nelson Mugambi. Optical Band Energy, Urbach Energy and Associated Band Tails of Nano Crystalline TiO_2 Films at Different Annealing Rates. *American Journal of Nanosciences*. Vol. 7, No. 1, 2021, pp. 28-34. doi: 10.11648/j.ajn.20210701.15

Received: January 24, 2021; **Accepted**: February 25, 2021; **Published**: March 9, 2021

Abstract: Increase in world population has led to more energy demand. Therefore, there is need for utilization of green and renewable energy. Dye sensitized solar cells (DSSCs) based on TiO_2 have attracted a lot of attention as an alternative source as compared to current silicon technology. In this study, TiO_2 thin films were deposited on doped fluorine tin oxide layer (FTO) glass substrates using sol-gel doctor blading technique. The films were annealed at different rates (1step, 2°C/min and 1°C/min) up to a temperature of 450°C followed by sintering at this temperature for 30 minutes. UV-VIS spectrophotometry was employed to probe the absorbance and reflectance of the films. It was found that, the optical parameters, such as the reflectance, the real (ε_1) and imaginary (ε_2) parts of dielectric constant, skin depth, Urbach energy and the energy gap; all depend on the annealing rate. The skin depth for the samples in visible region were found to increase from 6.319×10^{-5} to 11.968×10^{-5} cm^{-1} due to annealing. The Optical band energy (Eg) decreased from 5.04eV for as deposited film to 4.35eV at annealing rate of 1°C/min for direct allowed and from 2.76 to 2.56 eV for indirect transitions. Urbach tails in weak absorption region decreased with annealing rate. Urbach energies (Eu) were in the range of 432-505 meV for as deposited and annealed films. This was used to account for the disorder of the films. An inverse relation between Urbach energy and optical band energy as result of annealing rate was reported.

Keywords: Annealing Rate, Band Gap, Skin Depth and Urbach Energy

1. Introduction

Titanium IV oxide (TiO_2) in the recent decades is attracting much attention to many researchers due to its excellent chemical, thermal, optical and electrical properties. TiO_2 extensive investigations is due to its uses in various fields such as gas sensors [1], electronic materials [2], wet-type solar cells [3], electrochromic systems [4], antireflective coatings [5] and dye-sensitized solar cells [6]. TiO_2 in nature occurs in the structure of anatase, rutile and brookite [7]. The anatase phase can be obtained at temperatures below 800°C, which at higher temperatures transform to the more stable rutile structure [8]. The surface morphology is strongly affected by the annealing temperatures of TiO_2 thin films. The thin films have high transparency in the visible range and high opacity in the UV region [9]. The layer thickness of TiO_2 decreases with increase in annealing temperature attributed to densification of the titanium dioxide layer and evaporation of the carbonaceous material and absorbed water [9]. The highest refractive index obtained for anatase TiO_2 is 2.26 which increases to 2.57 with further annealing. This can be explained by crystalline structure development [10]. UV-VIS studies on optical absorption properties of TiO_2 has shown sharp absorption edges in the UV region and the absorption varying with annealing temperature. The absorption edge (in anatase) annealed at 450°C showed a red shift into the visible region [11]. The UV absorption peaks in

TiO_2 occurs due to band to band absorption [12, 13]. The hump in the visible region has been attributed to presence of Ti^{3+} or oxygen vacancies [14, 15] that bring about defect complex and form color centers [16, 17]. The band gap of TiO_2 films lowers with increase in annealing temperature which is associated with presence of defect bands in the band gap. An absorption tail (Urbach tails) is produced by these defect states which extends deep into the forbidden gap and the associated energy is the Urbach energy [18, 19].

The physical and chemical properties of the prepared materials depend very much on the technique applied for their fabrication. Preparation of TiO_2 thin films have been done using many techniques, which includes, cathodic electrodeposition [20, 21], Pulsed laser deposition [22], Mist plasma evaporation [23], electron beam evaporation [24], Metal organic chemical [25]. Doctor Blade is the most popular approach because it is simple, easy to scale up, cost effective and suitable for a large area processing [26]. UV – visible spectrophotometry has been used to characterize nanocrystalline TiO_2 thin films [27]. Optical measurements such as Reflectance and absorbance have been analysed using Scout software [28]. Optical band gap, Eg is calculated using Tauc's plot using absorption coefficient data obtained from scout software [29, 30]. Urbach energy and weak absorption tail energy is determined using absorption coefficient data [31]. In this work, allowed direct and indirect band gap, Urbach energy and associated Urbach tails were studied at different annealing rates.

2. Experimental Procedure

TiO_2 thin films were deposited on FTO (SnO_2: F) 7 Ω/sq, (Xinyan Technology Co. Limited, China) glass substrates using sol-gel technique. The TiO_2 (T/SP, 18% wt, 15-20nm was sourced from Solaronix, Switzerland) The prepared films were annealed at different rates using muffle furnace. The temperature was increased gradually at the up to 450°C followed by sintering for 30 minutes which is one step annealing. The other annealing rate was 1°C/min whereby the temperature was raised at a rate of 1 degree Celsius per minute up to 450°C followed sintering for 30 minutes, similar procedure was repeated for 2°C/min annealing rate. The optical reflectance and absorbance were measured in the wavelength range of 300-800 nm using double beam UV-Visible spectrophotometer (Shimadzu UV probe 1800, Japan). Values of absorption coefficient for all corresponding wavelength were obtained using SCOUT analysis [28]. Direct and indirect allowed optical band gaps were modelled using Tauc's relation [29]. Urbach energy and tails were obtained from absorption coefficients [31].

3. Result and Discussion

3.1. Reflectance

Figure 1 shows reflectance versus wavelength spectra for annealed TiO_2 films.

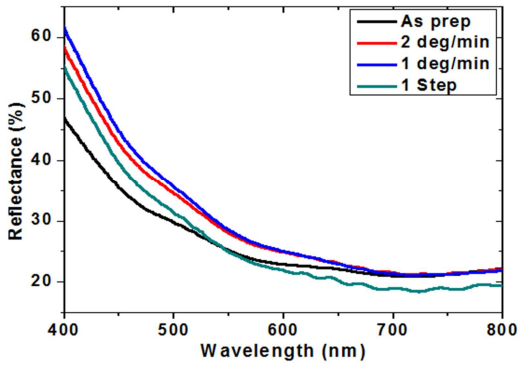

Figure 1. *A graph of Reflectance versus wavelength.*

Reflectance decreases gradually within the visible region. Room temperature deposited TiO_2 thin film illustrates only about 20% reflectance which can be useful for antireflection coating. The film with the lowest annealing rate (1°C/min) has the highest reflectance while 1 step (highest annealing rate) film has lowest reflectance. Based on literature, diffuse reflectance of TiO_2 nanoparticles has been studied. An increase in reflectance at higher annealing temperatures was observed due to decrease in crystallite sizes hence increase in surface area of particles to scatter light [18]. Further, a higher reflectance has been associated with a higher crystallinity and a higher thermal conductivity [19]. We therefore attribute an increase in reflectance as observed in figure 1 to improvement in crystallinity due to decrease in lattice imperfections and enhanced homogeneity due to annealing.

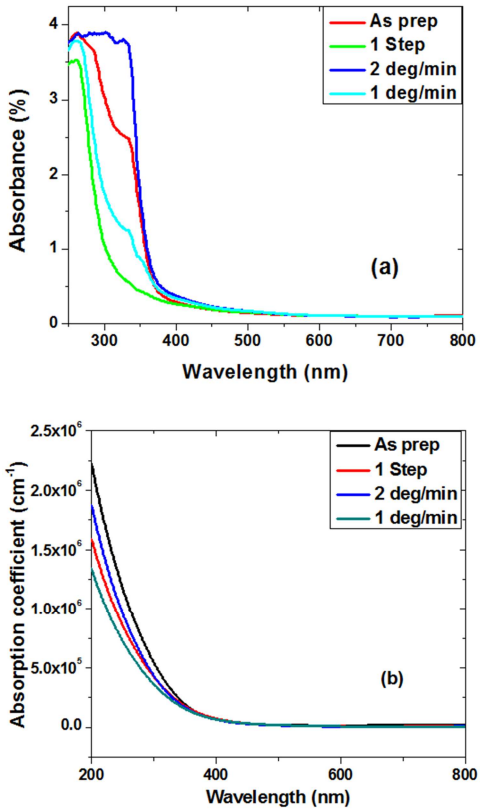

Figure 2. *Absorbance (a) and absorption coefficient (b) of as deposited and annealed TiO_2 films versus wavelength.*

3.2. Absorbance and Absorption Coefficient

Figure 2 (a) shows the absorbance and 2 (b) the absorption coefficient spectra in the range of 200-800 nm for TiO_2 thin films for as deposited and annealed. In the wavelength range of 250 nm to 380 nm, there is a significant increase in absorbance with decrease in annealing rate, this is due to high absorption of TiO_2 films in the ultraviolet region. Beyond a wavelength of 400 nm, the absorbance is fairly low and constant whereas the absorption edge tails are exponential, signifying the presence of localized states in the energy bandgap. The magnitude of tailing can be projected by plotting the absorption edge in terms of Urbach equation [32]. In the exponential edge region, the absorption edge provides a measure of the energy bandgap and the exponential tails dependence of the absorption coefficient [33, 34]. Therefore, lowering annealing rate leads to a reorganization and distribution of states from band to tail which is attributed to the improvement of crystallinity [18, 19].

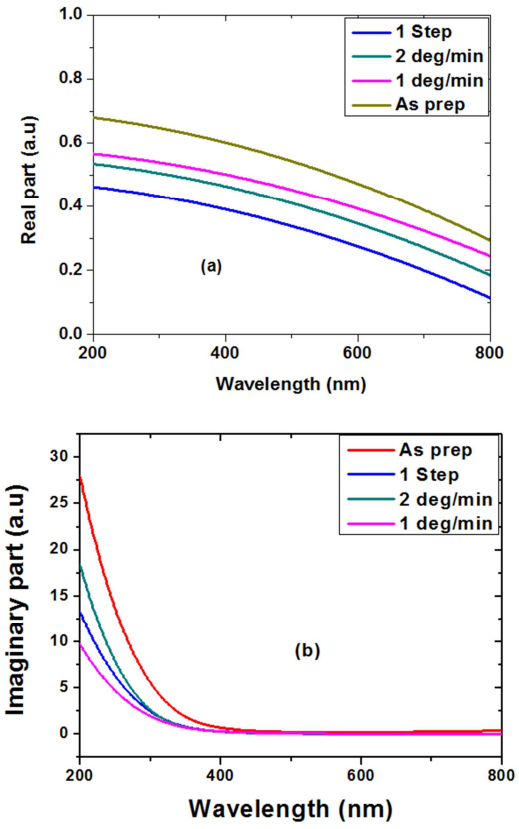

Figure 3. *Plot of the real part (a) and imaginary part (b) of the dielectric constant as a function wavelength for TiO_2 thin films for as deposited and annealed.*

3.3. Dielectric Constants

Figure 3 (a) and (b) represents the relationship between real and imaginary dielectric constants with wavelength for TiO_2 thin film for various annealing rates. They were calculated from equations (1) and (2).

$$\varepsilon_1 = n^2 - K^2 \quad (1)$$

$$\varepsilon_2 = 2nK \quad (2)$$

The ε_1 and ε_2 represent the amount of energy stored in dielectrics as polarization and loss energy respectively. Dielectric constants of annealed films were lower than that of as prepared. Real part dielectric increase with decreasing annealing rate and decreases with increasing wavelength. Imaginary part decreases sharply between 200nm to 400nm and remains fairly constant for all other wavelengths >400nm.

A greater ratio of ε_2 to ε_1 shows avery good low-loss dielectric of the thin film coatings having nature in the frequency range of interest. This is attributed to the intensification in the electron density of the films [35]. In general, the enhancement in crystallinity due to annealing of the films decreases the degree of electron scattering and thus increase the free-electron density [36, 37].

3.4. Skin Depth

The skin depth can take the value of one hundred to several thousand angstrom depending on the characteristics of the material. Skin depth (x) was calculated by the following equation [38].

$$x = \frac{\lambda}{2\pi k} \quad (3)$$

Figure 4 shows a plot of skin depth versus wavelength. It can be seen that at shorter wavelengths less than 500nm there is no significant change in skin depth values. This is due to equal probability in absorption in this region.

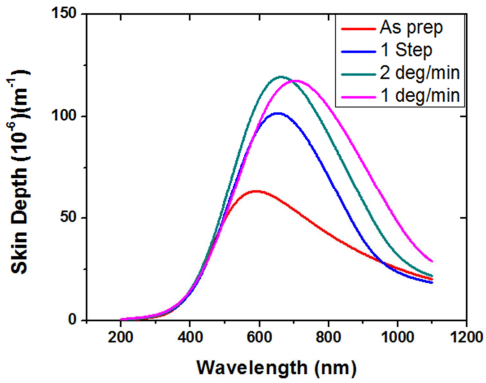

Figure 4. *Plot of skin depth for as prepared and annealed TiO_2 films.*

However, after wavelength, λ (cut off) (~525nm) the skin depth decreases for as deposited and annealed films whereas as deposited film has the lower skin depth values and film with lower annealing rates (1°C/min and 2°C) has higher values. The skin depth peaks for as prepared, 1 step, 2°C/min and 1°C/min were as shown in table 1.

Table 1. *Skin depth peaks.*

Annealing rate	Peak wavelength	Skin depth (x10^{-5}) (m^{-1})
As prepared	591	6.319
1 step	655	10.164
2°C/min	664	11.968
1°C/min	713	11.772

3.5. Direct Allowed and Indirect Allowed Optical Band Energy

The optical band gap energy, E_g was obtained from the absorption coefficient, α through Tauc's relations 4 and 5 for direct and indirect transitions [38, 39].

$$\alpha h\nu = B_1(h\nu - E_{g1})^2 \quad (4)$$

$$\alpha h\nu = B_2(h\nu - E_{g2})^{\frac{1}{2}} \quad (5)$$

where B_1 and B_2 are constants, α is the absorption coefficient, $h\nu$ is the photon energy and E_{g1}, E_{g2} are the direct and indirect band gaps, respectively. Figure 5 (a) and 5 (b) show the representation of the dependence of $(\alpha h\nu)^2$ and $(\alpha h\nu)^{\frac{1}{2}}$ respectively upon photon energy for as deposited and annealed TiO_2 films at different rates.

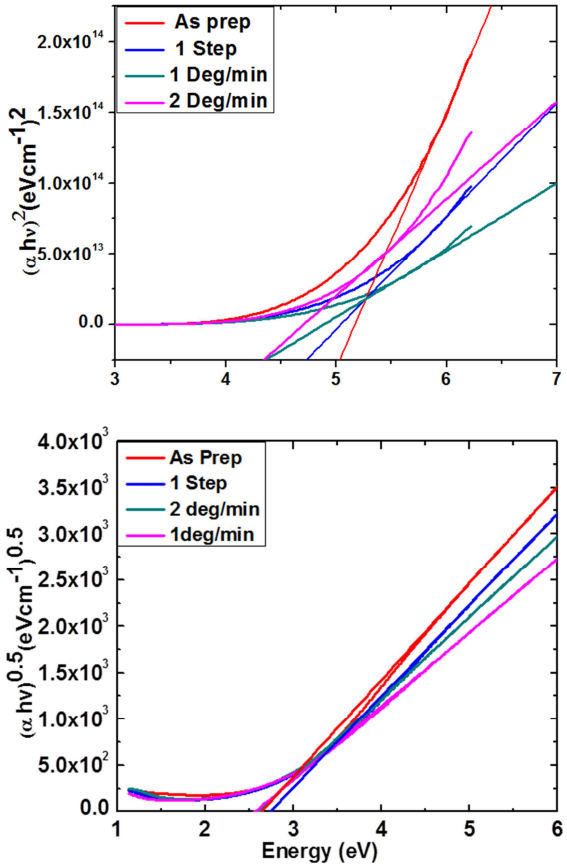

Figure 5. *(a) The variation of the $(\alpha h\nu^2$ with the photon energy and (b): The variation of $(\alpha h\nu)^{\frac{1}{2}}$ with increasing photon energy of TiO_2 thin-film samples at different annealing rates.*

Figure 5a shows the experimental data of a plot of $(\alpha h\nu)^2$ versus photon energy linear fit was extrapolated and the intercept determined the optical direct band gap, E_g. The optical allowed direct band gap energies were found to decrease from 5.04 to 4.35 eV for the present annealed TiO_2 films. While for indirect allowed band gap, E_{g2} extrapolation of the linear portion of the plot $(\alpha h\nu)^{\frac{1}{2}}$ versus photon energy decreased from 2.76 to 2.56 eV. These values are in good agreement with the data obtained for like phase [38-40]. It was further found that this decrease in E_g-values is as a result of the improvement of the crystallinity of films as well as the structure and the surface morphology of samples [41]. In the present work, the decrease in optical band gap is attributed to the oxygen defect band states formed in the band gap and increase of oxygen vacancies in the crystal lattice.

3.6. Urbach Energy (Eu) and Band Edge Absorption Tails

When a disorder arises during transition of electrons from top valence band to the bottom of conduction band, electrons encounter density of their states ρ (hν), where hν is the photon energy which result to tailing into the energy gap. This tail of ρ (hν) extending into the energy band gap is referred to as Urbach tail. Consequently, the energy associated with this tail is referred to as Urbach energy (E_u) which is due to tailing of absorption coefficient α (hν) in an exponential manner. Urbach energy is calculated as in equation 6:

$$\alpha(h\nu) = \alpha_0 exp(\frac{h\nu}{E_u}) \quad (6)$$

Where α_0 is a constant, hν is the photon energy and Eu is the Urbach energy.

In Figure 6, Region W represents the weak absorption region for as deposited and annealed TiO_2 films, U represents the urbach region and T represents the optical transitions from one extended state to another extended state. It is observed that all samples have an associated Urbach tail in region W.

The urbach tailing was observed to decrease with decrease in annealing rate, urbach tail of as prepared films is longest and that of 1degree/min annealing rate is the shortest. From literature, exponential tails are associated with low crystalline films, and disordered amorphous materials because of localized states [42, 43]. Therefore, it is evident that the energy below approximately 2.5eV is not sufficient to initiate a interband transition of electrons resulting to urbach tails in region W (weak absorption region).

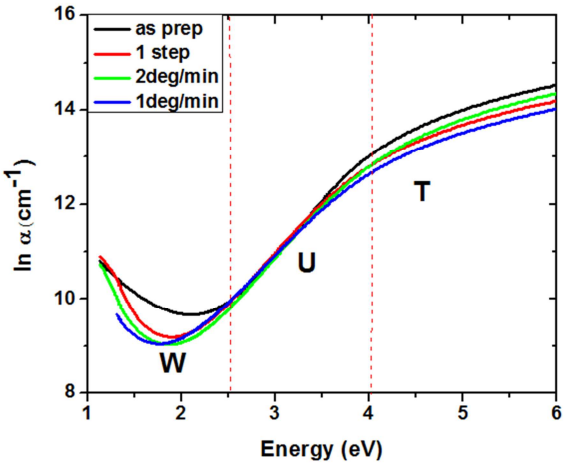

Figure 6. *ln (α) vs (hν) for TiO_2 thin films before and after annealing at different rates.*

Earlier work has associated this tailing of bands to lattice vibration due creation of sub-surface defects such as vacancies, vacancy-interstitial pairs and antisites [44]. We therefore,

attribute the tailing of bands to formation of oxygen vacancies due to annealing, whereas decrease in urbach tailing with decrease in annealing rate is due to improvement in crystallinity of the films. Urbach energy (E_u) was estimated by plotting ln (α) vs photon energy (hv) and fitting the linear portion of the curve with a straight line as shown in figure 7. From equation 6 reciprocal of the slope of the linear region yields the value of E_u. Estimated Urbach energies of TiO_2 films as deposited, 1 step, 2deg/min and 1 deg/min were 432meV, 464meV, 454meV and 505meV respectively. The values of urbach energies were correlated with optical band energies as shown in figure 8.

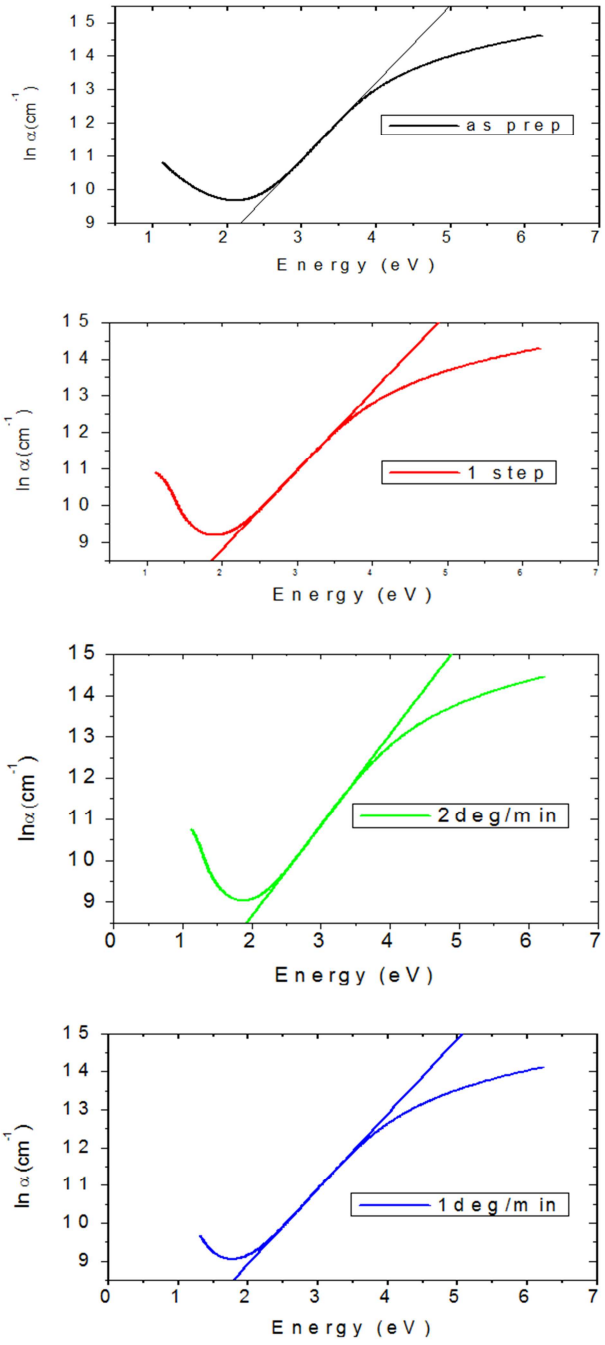

Figure 7. *Linear fit on ln (α) vs (hυ) for TiO_2 thin films at different annealing rates.*

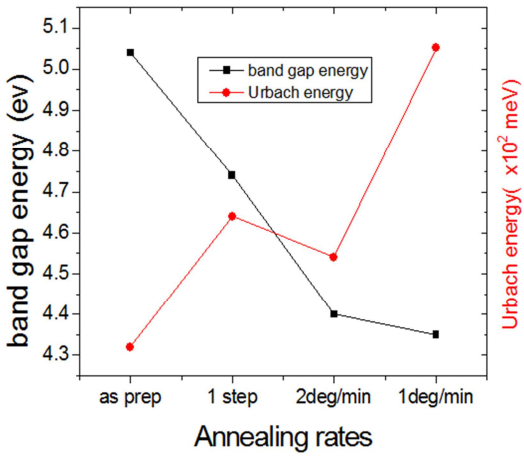

Figure 8. *Correlation between optical band energy and Urbach energy.*

We observe from figure 8 an increase in E_u from as prepared TiO_2 film to 1 step annealing rate followed by a decrease for 2 deg/min rate and an increase again at 1deg/min rate. Based on literature, the effect of annealing process on structural and optical properties has been studied [45]. XRD analysis by Shomara et al shows increase in annealing temperature gradually increases crystallite sizes, decreases lattice imperfections as well as enhancing nucleation and coalescence. However, localized tail states in amorphous semiconductors have been reported to arise from defects generated disorder. Increase in substrate temperature was also found to decrease associated E_u due to shuffling motion of atoms in randomly stacked polyhedra in an amorphous matrix. [42, 46]. As the temperature of the substrate increases, films were found to be more crystalline with increased band gap and reduced Urbach tail. Therefore, as observed in figure 8, all annealed films have a higher E_u than as prepared film which can be attributed to presence of localized states in annealed films. Decrease in E_u from 464meV to 454meV can be attributed to shift of films from amorphous to microcrystalline whereas the increase in Eu 454meV to 505meV at low annealing rate (1 deg/min) could be due creation of oxygen vacancies due to absorption in form of lattice vibrations. It has been reported a decrease in of optical band gap, E_g with the increase in annealing temperature [47]. Increased levels of localized states near conduction band and valence band is as a result of annealing [48]. These levels are ready to receive electrons and generate tails in the optical energy gap. Decrease in energy gap can be attributed to the increased size of particles in the films. Hence, we can associate the decrease in the band gap energy with increasing the annealing temperature to the lowering of interatomic spacing. Earlier studies on the effect of annealing temperature on structure, microstructure, morphology and optical properties of TiO_2 thin films revealed a nanocrystalline structure, uniform surface morphology and decreasing optical band gap with increasing annealing temperature [49]. As deposited TiO_2 films were found to be amorphous. The crystallinity of the tetragonal anatase phase improved after annealing at T > 693K [49]. The change from amorphous-to-polycrystalline nature has been reported to occur after annealing at about 400°C.

Band gap of the film decreased from 3.4 to 3.32 eV after annealing at 600°C [50]. A decrease in transmittance and optical energy band gap was reported with an increase in annealing temperature [51]. Studies on anatase TiO_2 thin films deposited by chemical bath deposition, revealed that increasing annealing temperature lead to improvement of the crystallinity quality of the films, increasing the urbach energy and the reduction of the band gap value [52].

4. Conclusion

TiO_2 thin films have been deposited using doctor blading technique and characterized using UV-VIS NIR spectroscopy. A stout dependence of reflectance, the real (ε_1) and imaginary (ε_2) parts of dielectric constant, skin depth, Urbach energy and the energy gap on annealing rate has been established. Variations in optical parameters have been associated from literature with changes in microstructure at different annealing rates giving rise to significant decrease in optical band-gap and increase in Urbach energy. Sub-surface defects of the films as manifested by the Urbach energy tails in the band-gap, can be used as a measure of disorder of the films. These observations indicate that a fine control over optical band-gap and microstructure of the films can be achieved via annealing rates. This can further lead to modification of TiO_2 to harness it for various optical applications.

References

[1] Lyson-Sypien, B., Czapla, A., Lubecka, M. (2013) Gas sensing properties of TiO_2–SnO_2 nanomaterials. *Sensor Actuators* 187, 445–454.

[2] Li, C. P., Wang, J. F., Su, W. B. (2003) Effect of sinter temperature on the electrical properties of TiO_2 based capacitor-varistors. *Material Letters* 57, 1400–1405.

[3] Michael, G. (2001) Sol–gel processed TiO2 films for photovoltaic applications. Journal of Sol Gel. *Science Technology* 22, 7–13.

[4] Tachibana, Y., Ohsaki, H., Hayashi, A. (2000). TiO_2–X sputter for high rate deposition of TiO_2. V*acuum*. 59, 836–843.

[5] Ben Naceur J., Gaidi M., Bousbih F., Mechiakh R. and Chtourou R. (2012) "Annealing effects on microstructural and optical properties of Nanostructured-TiO_2 thin films prepared by sol–gel technique", *Current Applied Physics*.

[6] Huang, M., Yu, S., Li, B. (2014). Influence of preparation methods on the structure and catalytic performance of SnO2-doped TiO_2 photocatalysts. *Ceram International* 40, 13305–13312.

[7] Chen Y. F., Lee C. Y., Yeng M. Y. and Chiu H. T. (2003). Preparing titanium oxide with various morphologies. *Materials Chemistry and Physics*. 81: 39–44.

[8] Palik E. D., (1991). Handbook of Optical Constants of Solids, vol. II, *Academic Press*, 795.

[9] Naceur J. B., Gaidi M., Bousbih F., Mechiakh R. and Chtourou R. (2012). Annealing effects on microstructural and optical properties of Nanostructured-TiO_2 thin films prepared by sole-gel technique. Current Applied *Physics* 12: 422-428.

[10] Wang X., Wu G., Zhou B. and Shen J. (2013). Optical Constants of Crystallized TiO_2 Coatings Prepared by Sol-Gel Process. *Materials*, 6, 2819-2830.

[11] Vasuki T, Saroja M, Venkatachalam M and Shankar, (2015). Synthesis and characterization of TiO2 thin film for photocatalytic degradation of textile dye effluent. *International Journal of Recent Scientific Research*. 4, 3511-3514.

[12] Choudhury, B., Borah, B., and Choudhury, A. (2013) Ce-Nd codoping effect on the structural and optical properties of TiO_2 nanoparticles, *Materials Science and Engineering B*, 178 (4), 239-247.

[13] Mo, S. D., and Ching, W. Y. Electronic and optical properties of three phases of titanium dioxide: Rutile, anatase, and brookite, Physics Rev. B 51 (19), 1 3023, 1995.

[14] T. Sekiya, K. Ichimura, M. Igarashi, S. Kurita, Absorption spectra of anatase TiO_2 single crystals heat treated under oxygen atmosphere, *Journal Physical Chemistry Solids*. 61 (8), 1237-1242, 2000.

[15] Liu, G., et al. Enhanced photoactivity of oxygen deficient anatase TiO_2 sheets with dominant {101} facets, *Journal of Physical Chemistry*. 113 (52), 21784–21788, 2009.

[16] Komaguchi, K., et al. Electron transfer reactions of oxygen species on TiO_2 nanoparticles induced by sub band gap illumination, *Journal Physical Chemistry*. 114 (2), 1240–1245, 2010.

[17] Kuznetsov, V. N., & Serpone, N. On the origin of spectral bands in the visible spectral bands in the visible absorption spectra light active TiO_2 specimens analysis and assignments, *Journal Physical Chemistry*. 113 (34), 15110–15123, 2009.

[18] Chiodo L., Lastra J. M., Iacomino A., Ossicini S., Zhao J., Petek H., Rubio A. (2010) Self-energy and excitonic effects in the electronic and optical properties of TiO_2 crystalline phases, *Physics Review* 82 (4), 045207.

[19] Boubaker K. (2011). A physical explanation to the controversial Urbach tailing universality, *The European Physics Journal Plus*, 126, 10.

[20] Natarajan C., Nogami G., *Journal of The Electrochemical Society* 143 (1996) 1547-1570.

[21] Karuppuchamy S., Nonomura K., Yoshida T., Sugiura T., Minoura H., Solid State Ionics. 151 (2002) 19-27.

[22] Garapon C., Champeaux C., Mugnier J., Panczer G., Marchet P., Catherinot A. and Jacquier B. (1996). Preparation of TiO_2 thin films by pulsed laser deposition for wave guiding applications Appl. Surf. Sci. 96-98 836-841.

[23] Huang H., Yao X., J. Cryst. Growth 268 (2004) 564-567.

[24] Wang F. X., Hwangbo C. K., Jung B. Y., Lee J. H., Park B. H., Kim N. Y., Surf. Coat. Technol. 201 (2007) 5367-5370.

[25] Antunes R. A., Deoliveira M. C. L., Pillis M. F., Int. J. Electrochem. Sci. 8 (2013) 1487–1500.

[26] Benjamin M. J., Simon W. M., and James M. N. (2018) "Effect of Annealing Rates on Surface Roughness of TiO_2 Thin films." Journal of Materials Physics and Chemistry, 6 (2): 43-46.

[27] Sta I, Jlassi M, Hajji M, Boujmil M. F, and Jerbi R. (2014). Structural and optical properties of TiO_2 thin films prepared by spin coating. Journal of Sol-Gel Science and Technology 72: 421-427.

[28] Theiss, W. (2000). Scout thin films analysis software handbook, edited by Theiss M (Hand and Software Aachen German) www.mtheiss.com.

[29] Sharma N, Prabakar K, Ilango S, Dash S and Tyagi A K (2015). Application of dynamic scaling theory for growth kinetic studies of AlN-thin films deposited by ion beam sputtering in reactive assistance of nitrogen plasma, Applied Surface Science 347: 875-9.

[30] Sharma N, Ilango S, and Dash S and Tyagi A K 2015 XPS studies on AlN thin films grown by ion beam sputtering in reactive assistance of N+ /N2+ ions: Substrate temperature induced compositional variations arXiv: 1510.00541.

[31] Boubaker K 2011 A physical explanation to the controversial Urbach tailing universality The European Physical Journal Plus 126 1-4.

[32] Urbach, F., The Long-Wavelength Edge of Photographic Sensitivity and of the Electronic Absorption of Solids, Phys. Rev., 92, 1324-1325 (1953).

[33] Tauc, J., Amorphous and Liquid Semiconductors, Plenum Press, New York, (1974).

[34] Tauc, J., R. Grigorovici and Vancu, A. Optical Properties and Electronic Structure of Amorphous Germanium, Phys. Status Solidi, 15, 627-637 (1966).

[35] M. Balkanski, R. F. Wollis; "Semiconductor physics and application", Oxford University Press (2000).

[36] C. Fournier, O. Bamiduro, H. Mustafa, R. Mundle, R. B. Konda, F. Williams and A. K. Pradhan, Semiconductor Science and Technology., 2008, 23, 085019.

[37] Y. Kim and J. Y. Leem, Phys. B, 2015, 476, 71–76.

[38] Akl, A. A. Kamal H., Abdel-Hady K. (2006) "Fabrication and characterization of sputtered titanium dioxide films", *Applied Surface Science*, 252: 8651–8656.

[39] Cheng, W. X., Ding, A. L., Qiu, P. S., He, X. Y. and Zheng, X. S. H. (2003). Optical and dielectric properties of highly oriented (Zr0.8, Sn0.2) TiO4 thin films prepared by rf magnetron sputtering, Applied Surface Science 214: 136-142.

[40] Tauc, J. in: J. Tauc (Ed.), Amorphous and Liquid Semiconductors, Plenum Press, London and New York, 1974.

[41] El-Nahass, M. M., Soliman, H. S., El-Denglawey, A. (2016). Absorption edge shift, opticalconductivity, and energy loss function of nano thermal-evaporated N-typeanatase TiO_2 films. Appl Phys A; 122: 775.

[42] Mathews, N. R., Morales, E. R., Cortés-Jacome, M. A., & Antonio, J. T. (2009). TiO_2 thin films–Influence of annealing temperature on structural, optical and photocatalytic properties. Solar Energy, 83 (9), 1499-1508.

[43] Wibowo, K. M., Sahdan, M. Z., Asmah, M. T., Saim, H., Adriyanto, F., & Hadi, S. (2017), August). Influence of Annealing Temperature on Surface Morphological and Electrical Properties of Aluminum Thin Film on Glass Substrate by Vacuum Thermal Evaporator. In IOP Conference Series: Materials Science and Engineering (Vol. 226, No. 1, p. 012180). IOP Publishing.

[44] Sharma N., Sharma S., Prabakar K., Amirthapandian S., Ilango S., Dash S. and Tyagi A. K. Optical band gap and associated band-tails in nanocrystalline AlN thin films grown by reactive IBSD at different substrate temperatures Material Science Group, Indira Gandhi Centre for Atomic Research 603102.

[45] Al-Shomara, S. M., Alahmad W. R. (2019), Annealing temperature effect on structural, optical and photocatalytic activity of nanocrystalline TiO_2 films prepared by sol-gel method used for solar cell application, Digest Journal of Nanomaterials and Biostructures, 14, 617-625.

[46] Hasan M. M., Haseeb A. S. M. A., Saidur R., and Masjuki H. H. (2009). Effects of Annealing Treatment on Optical Properties of Anatase TiO_2 Thin Films. Journal of Nuclear Science and Technology.

[47] Sankar S. and Gopchandran, K. G (2009). Effect of annealing on the structural, electrical and optical properties of nanostructured TiO_2 thin films. Crystal Research and Technology. 44: 989-994.

[48] Pawar, S. Chougule, M. Godse, P. Jundale, D. Pawar S. Raut, B. and Patil, V. (2011). Effect of annealing on structure, morphology, electrical and optical properties of nanocrystalline TiO_2 thin films. Journal of Nano- Electron Physics. 3: 185–192.

[49] Khan F. U., Zubair M., Ansar M. Z., Alamgir M. K., Nadeem S. (2016) "Effect of Annealing Temperature on the Structural and Optical Properties of TiO_2 Thin Film Prepared by Sol-gel Method", *Journal of Scientific Research,* 8 (3), 267-272.

[50] Mathews, N. R. Morales, E. R. Corte´s-Jacome, M. A., and Toledo Antonio J. A., (2009) TiO_2 thin films – Influence of annealing temperature on structural, optical and photocatalytic properties, Solar Energy 83: 1499–1508.

[51] Atefeh T. and Davood R. (2016). The annealing temperature dependence of anatase TiO_2 thin films prepared by the electron-beam evaporation method, Semiconductor Science and Technology. 31: 12.

[52] El Fanaoui1, A. Taleb, A. El Hamri, E. Boulkaddat, L. Kirou, H. Atourki, L. Ihlal A. and Bouabid K. (2016) Effect of heat treatment on TiO_2 thin films properties, Journal of Material Environmental Science, 7 (3) 907-914.